Ion Pairing of $[Fe_3(\mu\text{-}H,\mu\text{-}CO)(CO)_{10}]^-$ with $H_2NR_2^+$ Cations

C. K. Chen, C. H. Cheng,* and T. H. Hseu*

Department of Chemistry and The Institute of Life Science, National Tsing Hua University, Hsinchu, Taiwan 300, Republic of China

Received August 14, 1986

The bridging ν_{CO} of $[H_2R_2N]^+[HFe_3(CO)_{11}]$ (R = Et, *n*-Bu) appears at 1550 cm^{-1} in the solid state, at ~1650 cm^{-1} in benzene or chloroform, and at ~1745 cm^{-1} in THF. The corresponding ν_{CO} of the $H_2(i\text{-}Pr)_2N^+$ salt also occurs at about the same position as that of the $H_2R_2N^+$ salt in the same solvent. In the solid state, however, in addition to a new band at 1883 cm^{-1} in the terminal CO region the bridging ν_{CO} appears at 1650 cm^{-1}. There is no similar terminal band in the other salts. The crystal structure of $[H_2(i\text{-}Pr)_2N][HFe_3(CO)_{11}]$ was determined by a single-crystal diffraction method. The structure details indicate that the bridging CO group and one of the terminal CO groups are each hydrogen-bonded to an acidic proton on two separate cations. The hydrogen bonding provides a basis for the understanding of the ν_{CO} change of $HFe_3(CO)_{11}^-$ with its environment. The bridging ν_{CO} at 1740, 1650, and 1550 cm^{-1} is explained as the consequence of the formation of none, one, and two hydrogen bonds, respectively, between the bridging CO and the countercations.

Introduction

Ion pairing of metal carbonylates with their countercations has attracted considerable interests in recent years. The results of the studies have shown that the coordination of alkali ions to the carbonyl oxygens greatly accelerate the alkyl migration in $RFe(CO)_4^-$[1-3] and increase the reactivity of $HFe(CO)_4^-$ toward oxygen molecule.[4] On the other hand, the hydrogen bonding between the bridging CO of $HFe_3(CO)_{11}^-$ and $HNEt_3^+$ reduces the CO scrambling rate in the carbonyl anion.[5]

While extensive studies on the ion pairing of mononuclear metal carbonylates have been conducted,[1-4,6] there is much less work concerning the same phenomena in clusters.[5,7,8] Our interests in the ion pairing of metal cluster anions have been focused on the interaction of $HFe_3(CO)_{11}^-$ with its countercations and with solvents. The cluster anion has a single bridging CO group that in most cases is the center for ion pairing and solvation. The IR absorption frequency of this CO group appears in a region that is not interfered by most solvent absorptions and by terminal CO absorptions. These unique features enable us to look into the details of the interactions of the iron carbonylate with its environment by measuring the CO frequency change. In a previous paper,[8] we had shown that $MHFe_3(CO)_{11}$ (M = alkali metal) exists as ion pairs in the solid state and in ether and dioxane, but the salts dissociate partially in THF solution and both contact ion pairs and less associated forms are present. In more polar solvents, the alkali salts exist only as less associated forms. However, the interaction between the bridging CO and the acidic protons on the solvent molecules becomes important. A recent study on the ion pairing of $HFe_3(CO)_{11}^-$ and the analogous $HRu_3(CO)_{11}^-$ with PPN^+ and NEt_4^+ showed that these salts in solutions form contact ion pairs and less associated species that may be distinguished from each other in the IR spectra.[9] A brief investigation on the interaction of $HNEt_3^+$ with $HFe_3(CO)_{11}^-$ also had been reported previously.[5] In this paper, we wish to present some novel examples of the ion pairing of metal carbonylates in the solid state and solutions that exhibit dramatic change in the CO frequencies with the environment. The systems investigated are several of the dialkylammonium salts of the $HFe_3(CO)_{11}$ anion. Moreover, the X-ray structure determination of one of the salts is also reported. The results give direct evidence for the contact ion pairing of the $HFe_3(CO)_{11}^-$ anion with its countercation in the solid state. Although the ion pairing of a large number of metal anions has been investigated, there are only a few mononuclear systems[10-14] that provide crystal structure evidence for such behavior. The present structure is believed to be the first example describing the interaction of a cation and metal carbonyl cluster anion in the crystalline state.

Experimental Section

All experiments were carried out under an atmosphere of nitrogen by using modified Schlenk techniques. IR spectra were recorded on a Jasco 100 spectrophotometer.

Iron pentacarbonyl (Strem) was used as purchased, while $KHFe_3(CO)_{11}$ was prepared according to the method reported previously by us.[8] $H_2Et_2N^+Cl^-$, $H_2(n\text{-}Bu)_2N^+Cl^-$, and $H_2(i\text{-}Pr)_2N^+Cl^-$ were obtained by the addition of a stoichiometric amount of hydrochloric acid to the corresponding dialkylamine in methanol followed by evaporation of the solution.

Preparation of Dialkylammonium *triangulo*-(μ-Carbonyl)decacarbonyl(μ-hydrido)triferrate(1-), $[H_2R_2N][HFe_3(CO)_{11}]$. To 1.00 g of $KHFe_3(CO)_{11}$ in 10 mL of water was added 1.1 equiv of dialkylammonium chloride in a

(1) Collman, J. P.; Finke, R. G.; Cawse, J. N.; Branman, J. I. *J. Am. Chem. Soc.* **1978**, *100*, 4766.
(2) Mclain, S. J. *J. Am. Chem. Soc.* **1983**, *105*, 6355.
(3) (a) Powell, J.; Gregg, M.; Kuksis, A.; Meindl, P. *J. Am. Chem. Soc.* **1983**, *105*, 1064. (b) Powell, J.; Kuksis, A.; May, C. J.; Nyburg, S. C.; Smith, S. J. *J. Am. Chem. Soc.* **1981**, *103*, 5941.
(4) Darensbourg, M.; Barros, H.; Borman, C. *J. Am. Chem. Soc.* **1977**, *99*, 1647.
(5) Wilkinson, J.; Todd, L. J. *J. Organomet. Chem.* **1976**, *118*, 199.
(6) Kao, S. C.; Darensbourg, M. Y.; Schenk, W. *Organometallics* **1984**, *3*, 871.
(7) Collman, J. P.; Finke, R. G.; Matlock, P. L.; Wahren, R.; Komoto, R. G.; Brauman, J. I. *J. Am. Chem. Soc.* **1978**, 100, 1119.
(8) Chen, C. K.; Cheng, C. H. *Inorg. Chem.* **1983**, *22*, 3378.
(9) Schick, K.-P.; Jones, N. L.; Sekula, P.; Boag, N. M.; Labinger, J. A.; Kaesz, H. D. *Inorg. Chem.* **1984**, *23*, 2204.
(10) Chin, H. B.; Bau, R. *J. Am. Chem. Soc.* **1976**, *98*, 2434.
(11) Teller, R. G.; Finke, R. G.; Collman, J. P.; Chin, H. B.; Bau, R. *J. Am. Chem. Soc.* **1977**, *99*, 1104.
(12) Calderazzo, F.; Fachinetti, G.; Marchetti, F. *J. Chem. Soc., Chem. Commun.* **1981**, 181.
(13) Fachinetti, G. F.; Floriani, C.; Zanazzi, P. F.; Zanzari, A. R. *Inorg. Chem.* **1978**, *17*, 3002.
(14) Schlussler, D. P.; Robinson, W. R.; Edgell, W. F. *Inorg. Chem.* **1974**, *13*, 153.

0276-7333/87/2306-0868$01.50/0

Table I. Fractional Coordinates ($\times 10^4$) for the Non-Hydrogen Atoms of $[H_2(i\text{-}Pr)_2N][HFe_3(CO)_{11}]$

atom	x/a	y/b	z/c
Fe(1)	2117 (2)	1301 (1)	-3666 (1)
Fe(2)	293 (1)	627 (1)	-2925 (1)
Fe(3)	-81 (2)	1895 (1)	-3066 (1)
C(11)	3723 (17)	885 (7)	-3654 (11)
C(12)	2132 (11)	905 (6)	-2177 (9)
C(13)	1749 (15)	1458 (7)	-5236 (12)
C(14)	2894 (13)	2032 (6)	-3182 (10)
C(21)	876 (14)	-145 (6)	-2820 (11)
C(23)	-195 (12)	641 (7)	-1576 (10)
C(24)	-1410 (13)	455 (6)	-3937 (12)
C(31)	-827 (16)	1714 (8)	-4561 (12)
C(32)	19 (13)	2696 (6)	-3397 (10)
C(33)	1008 (14)	1982 (7)	-1573 (11)
C(34)	-1777 (15)	1876 (7)	-2704 (13)
O(11)	4813 (11)	614 (6)	-3534 (11)
O(12)	2998 (9)	844 (4)	-1258 (7)
O(13)	1631 (13)	1509 (6)	-6191 (8)
O(14)	3531 (11)	2491 (5)	-2868 (8)
O(21)	1323 (12)	-660 (5)	-2715 (9)
O(23)	-485 (11)	633 (5)	-693 (8)
O(24)	-2467 (10)	309 (6)	-4544 (9)
O(31)	-1426 (12)	1673 (6)	-5521 (8)
O(32)	-7 (14)	3214 (5)	-3661 (9)
O(33)	1634 (11)	2056 (5)	-646 (7)
O(34)	-2779 (12)	1886 (8)	-2449 (11)
N	4477 (9)	1322 (5)	970 (7)
C(1)	4511 (13)	792 (6)	1865 (11)
C(2)	5110 (19)	1071 (8)	3068 (11)
C(3)	2962 (16)	654 (9)	1687 (12)
C(4)	5869 (12)	1531 (8)	766 (11)
C(5)	5643 (19)	2142 (10)	72 (15)
C(6)	6481 (16)	988 (10)	165 (15)

minimum amount of water. The precipitate was filtered, washed by distilled water, and then dried in vacuo to give the desired product. The presence of $HFe_3(CO)_{11}^-$ in these salts were identified by comparing their CO stretching frequencies and the chemical shift of the hydride (δ -14.94 in Me_2SO-d_6) with the corresponding data of the known $(HNEt_3)[HFe_3(CO)_{11}]$, while the existence of the dialkylammonium cations was confirmed by the ^1H NMR spectra of these complexes in Me_2SO-d_6.

Structure Determination of $[H_2(i\text{-}Pr)_2N][HFe_3(CO)_{11}]$. Crystals suitable for crystallographic measurements were obtained from benzene–hexane mixture. The compound crystallizes in the monoclinic space group $P2_1/c$ with a = 9.635 (4) Å, b = 21.182 (7) Å, c = 11.897 (5) Å, and β = 104.01 (3)°. The density calculated for four molecules per unit cell is 1.632 g cm^{-3}. All crystallographic measurements were made on a Nonius CAD-4F automatic diffractometer with Zr-filtered Mo Kα radiation (λ = 0.710 69 Å).

Intensity data were collected at room temperature with use of a θ–2θ scan technique. The intensities of three standard reflections were remeasured periodically and were used to rescale all the data by use of a linear interpolation procedure. Intensity data from azimuthal rotation about the two strong reflections 200 and 080 were used for the absorption correction[15] (μ = 19.3 cm^{-1}). Of a total of 5583 independent reflections with those $2\theta < 55°$ ((sin θ)/$\lambda \leq 0.65$) collected, 2956 were found to have intensities greater than 3 times their estimated standard deviations. Only these reflections were used in the subsequent analysis.

The structure was solved by the heavy-atom method and refined by the full-matrix least-squares method. The function minimized was $\sum w(|F_o| - |F_c|)^2$ with the weighing scheme given by Stout and Jensen.[16] The atomic scattering factors used were all taken from ref 17, with that of Fe corrected for anomalous dispersion. Except the bridging H atom, the positions of the hydrogen atoms were calculated with C–H = 0.95 Å, N–H = 0.9 Å, and a tetrahedral angle of 109.50°. The positional and isotropic thermal parameters of all H atoms were included in the calculation but not refined. The final refinement with anisotropic thermal parameter for non-hydrogen atoms led to values of R and R_w of 0.076 and 0.069, respectively, where $R_w = (\sum w(|F_o| - |F_c|)^2/\sum wF_o^2)^{1/2}$ and $R = \sum||F_o| - |F_c||/\sum|F_o|$. The final atomic coordinates are given in Table I. One perspective view of the $HFe_3(CO)_{11}^-$ is shown in Figure 1. A crystal packing diagram with bonding viewed along the b axis is presented in Figure 2. Selected bond distances and angles are listed in Table II. Tables of anistropic thermal parameters, coordinates of the hydrogen atoms, and observed and calculated structure factors are available; see the paragraph at the end of the paper regarding supplementary material.

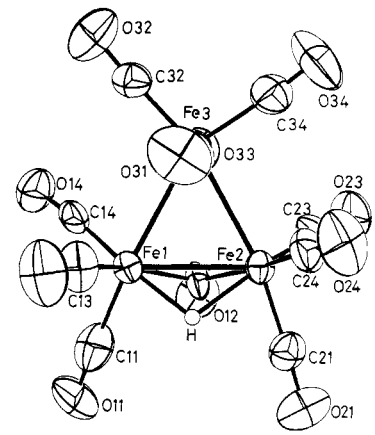

Figure 1. A perspective view of the structure of the anion in $[H_2(i\text{-}Pr)_2N][HFe_3(CO)_{11}^-]$.

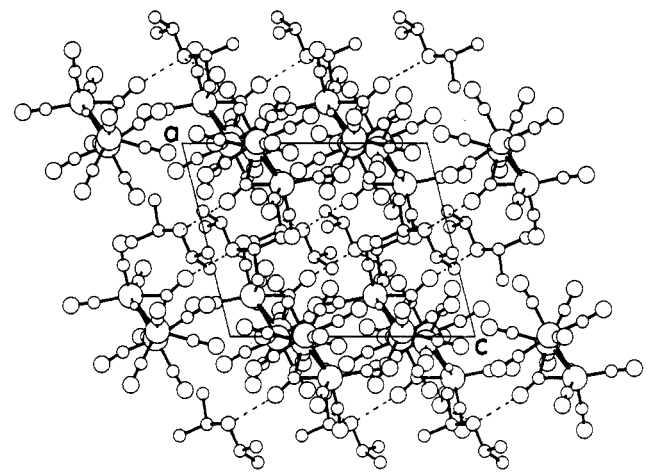

Figure 2. Crystal packing diagram of $[H_2(i\text{-}Pr)_2N][HFe_3(CO)_{11}]$ viewed along the b axis (hydrogen bonds are indicated by dashed lines).

Results and Discussion

Variations of the CO Frequencies of $HFe_3(CO)_{11}^-$ with Its Environment. The bridging CO frequencies of the dialkylammonium salts of $HFe_3(CO)_{11}^-$ changed dramatically with the countercations and the solvents used. In the solid state, the absorption frequency of $H_2Et_2N^+$ and $H_2(n\text{-}Bu)_2N^+$ salts appears at an extremely low value of 1550 cm^{-1} that is nearly 200 cm^{-1} lower than its highest absorption frequency of 1745 cm^{-1} in THF. The difference in the CO frequency change is believed to be the largest ever reported in the ion pairing studies of metal carbonylates. As the salts dissolve in chloroform or benzene, the bridging CO frequency increases to ca. 1650 cm^{-1} from the value of 1550 cm^{-1} in the solid state. The frequency further moves up to around 1740 cm^{-1} in THF and in

(15) North, A. C. T.; Philips, D. C.; Mathews, F. S. *Acta Crystallogr., Sect. A: Cryst. Phys., Diffr. Theor. Gen. Crystallogr.* **1968**, *A24*, 351.
(16) Stout, G. H.; Jensen, L. *X-ray Structure Determination*; Macmillan: New York, 1968, P 457.
(17) *International Table for X-ray Crystallography*; Kynoch Press: Birmingham, 1962; Vol. III, pp 201–203.

Table II. Bond Distances (Å) and Bond Angles (deg) of $[H_2(i\text{-}Pr)_2N][HFe_3(CO)_{11}]$

	Fe_3 Triangle		
Fe(1)–Fe(2)	2.579 (2)	Fe(2)–Fe(1)–Fe(3)	61.7 (1)
Fe(1)–Fe(3)	2.704 (3)	Fe(1)–Fe(2)–Fe(3)	61.4 (1)
Fe(2)–Fe(3)	2.709 (3)	Fe(1)–Fe(3)–Fe(2)	56.9 (1)
	Carbonyl Groups		
	$Fe(1)–(CO)_3$		
Fe(1)–C(11)	1.778 (16)	Fe(2)–Fe(1)–C(11)	112.7 (5)
Fe(1)–C(13)	1.845 (14)	Fe(2)–Fe(1)–C(13)	117.7 (5)
Fe(1)–C(14)	1.755 (12)	Fe(2)–Fe(1)–C(14)	130.4 (5)
C(11)–O(11)	1.175 (20)	Fe(3)–Fe(1)–C(11)	164.7 (4)
C(13)–O(13)	1.119 (17)	Fe(3)–Fe(1)–C(13)	102.3 (5)
C(14)–O(14)	1.162 (16)	Fe(3)–Fe(1)–C(14)	78.6 (4)
		Fe(1)–C(11)–O(11)	173.7 (12)
C(11)–Fe(1)–C(13)	92.9 (6)	Fe(1)–C(13)–O(13)	172.9 (14)
C(11)–Fe(1)–C(14)	97.7 (6)	Fe(1)–C(14)–O(14)	173.5 (12)
C(13)–Fe(1)–C(14)	97.8 (6)		
	$Fe(2)–(CO)_3$		
Fe(2)–C(21)	1.725 (13)	Fe(1)–Fe(2)–C(21)	108.2 (5)
Fe(2)–C(23)	1.779 (13)	Fe(1)–Fe(2)–C(23)	130.6 (4)
Fe(2)–C(24)	1.822 (12)	Fe(1)–Fe(2)–C(24)	117.7 (5)
C(21)–O(21)	1.168 (17)	Fe(3)–Fe(2)–C(21)	168.8 (5)
C(23)–O(23)	1.157 (17)	Fe(3)–Fe(2)–C(23)	88.8 (5)
C(24)–O(24)	1.139 (15)	Fe(3)–Fe(2)–C(24)	94.2 (4)
		Fe(2)–C(21)–O(21)	177.1 (11)
C(21)–Fe(2)–C(23)	95.9 (7)	Fe(2)–C(23)–O(23)	117.8 (12)
C(21)–Fe(2)–C(24)	94.8 (6)	Fe(2)–C(24)–O(24)	175.7 (12)
C(23)–Fe(2)–C(24)	101.9 (6)		
	$Fe(3)–(CO)_4$		
Fe(3)–C(31)	1.791 (14)	Fe(1)–Fe(3)–C(31)	77.9 (5)
Fe(3)–C(32)	1.749 (13)	Fe(1)–Fe(3)–C(32)	107.6 (5)
Fe(3)–C(33)	1.841 (12)	Fe(1)–Fe(3)–C(33)	90.1 (5)
Fe(3)–C(34)	1.788 (16)	Fe(1)–Fe(3)–C(34)	150.8 (5)
C(31)–O(31)	1.151 (16)	Fe(2)–Fe(3)–C(31)	82.2 (5)
C(32)–O(32)	1.140 (17)	Fe(2)–Fe(3)–C(32)	164.0 (5)
C(33)–O(33)	1.133 (14)	Fe(2)–Fe(3)–C(33)	90.2 (5)
C(34)–O(34)	1.080 (21)	Fe(2)–Fe(3)–C(34)	94.5 (5)
		Fe(3)–C(31)–O(31)	170.2 (15)
C(31)–Fe(3)–C(32)	90.9 (7)	Fe(3)–C(32)–O(32)	175.3 (11)
C(31)–Fe(3)–C(33)	167.9 (7)	Fe(3)–C(33)–O(33)	176.8 (13)
C(31)–Fe(3)–C(34)	93.7 (7)	Fe(3)–C(34)–O(34)	176.7 (15)
C(32)–Fe(3)–C(33)	94.1 (6)		
C(32)–Fe(3)–C(34)	100.4 (7)		
C(33)–Fe(3)–C(34)	96.3 (6)		
	Bridging Groups		
Fe(2)–C(12)	1.875 (10)	C(12)–Fe(1)–HFe	59.5
Fe(1)–C(12)	1.957 (11)	C(12)–Fe(2)–HFe	60.8
Fe(2)–HFe	1.652	C(12)–Fe(1)–C(11)	88.0 (6)
Fe(1)–HFe	1.610	C(12)–Fe(1)–C(13)	162.0
C(12)–O(12)	1.211 (12)	C(12)–Fe(1)–C(14)	99.9 (5)
		C(12)–Fe(2)–C(21)	90.5 (6)
Fe(1)–HFe–Fe(2)	104.4	C(12)–Fe(2)–C(23)	89.6 (5)
Fe(1)–C(12)–Fe(2)	84.6 (4)	C(12)–Fe(2)–C(24)	166.7 (6)
Fe(1)–C(12)–O(12)	135.7 (9)	Fe(2)–Fe(1)–C(12)	46.4 (3)
Fe(2)–C(12)–O(12)	139.5 (10)	Fe(3)–Fe(1)–C(12)	78.2 (3)
Fe(1)–HFe–C(12)	69.9	Fe(1)–Fe(2)–C(12)	49.1 (4)
Fe(2)–HFe–C(12)	65.7	Fe(3)–Fe(2)–C(12)	79.3 (4)
	Counterion		
N–C(1)	1.542 (16)	C(1)–N–C(4)	117.4 (9)
N–C(4)	1.487 (16)	C(2)–C(1)–C(3)	112.7 (13)
C(1)–C(2)	1.527 (18)	C(2)–C(1)–N	107.8 (10)
C(1)–C(3)	1.534 (20)	C(3)–C(1)–N	106.1 (10)
C(4)–C(5)	1.522 (26)	C(5)–C(4)–C(6)	113.7 (14)
C(4)–C(6)	1.545 (26)	C(5)–C4)–N	109.0 (11)
		C(6)–C(4)–N	108.3 (12)
	H Bonding		
N···O(12)[a]	2.873 (11)	O(12)···HN(2)–N	171.6
N···O(14)[b]	3.110 (15)	O(14)···HN(1)–N	166.8
HN(2)···O(12)[a]	1.932		
HN(1)···O(14)[b]	2.177		

[a] x, y, z. [b] $x, {}^1/_2 - y, {}^1/_2 + z$.

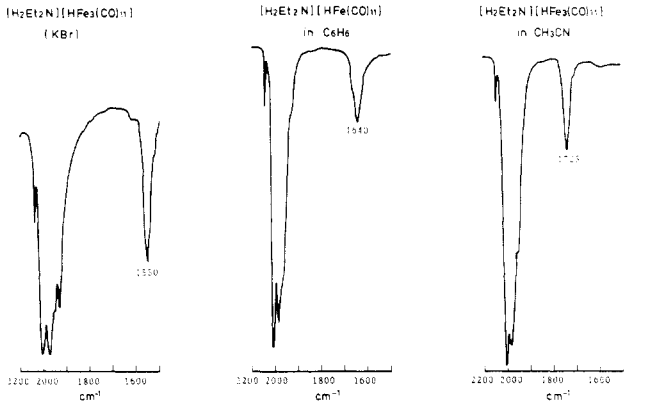

Figure 3. The carbonyl absorption spectra of $[H_2(Et)_2N][HFe_3(CO)_{11}]$ in the solid state and solutions.

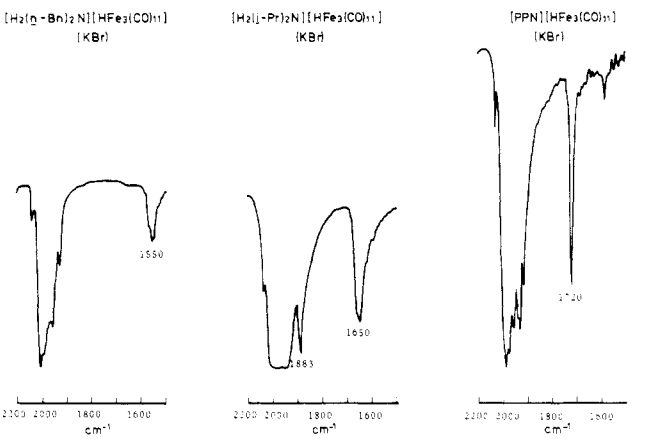

Figure 4. The carbonyl absorption spectra of $HFe_3(CO)_{11}^-$ with various cations in the solid state.

acetonitrile (Figure 3). On the other hand, the corresponding bridging CO frequency of the $H_2(i\text{-}Pr)_2N^+$ salt appears at 1650 cm^{-1} in the solid state as shown in Figure 4, but one of the terminal CO absorptions occurs at 1883 cm^{-1}. This absorption is at least 20 cm^{-1} lower in frequency than the lowest terminal CO absorption of the other $HFe_3(CO)_{11}^-$ salts presented in Figures 3 and 4. Interestingly, in benzene or chloroform, the bridging CO frequency remains at approximately the same position as in the solid state, but the band at 1883 cm^{-1} disappears. In THF, the bridging CO frequency shifts to 1745 cm^{-1}, the same position as that of the other $HFe_3(CO)_{11}^-$ salts in the same solvent.

A comparison of the CO frequencies of a number of $HFe_3(CO)_{11}^-$ salts is given in Table III. All of the bridging CO frequencies fall into three distinguished regions, that is, 1550, 1650, and 1735 cm^{-1}, with a deviation of ± 10 cm^{-1}.

Crystal Structure of $[H_2(i\text{-}Pr)_2N][HFe_3(CO)_{11}]$. In an effort to interpret the variation of CO frequencies of the iron carbonylate with the countercations and solvents, the structure of one of the salts, $[H_2(i\text{-}Pr)_2N][HFe_3(CO)_{11}]$, was determined by single-crystal X-ray diffraction methods. The basic structure of the $HFe_3(CO)_{11}^-$ anion from the present study (Figure 1) is in agreement with that of the $(HEt_3N)[HFe_3(CO)_{11}]$ examined previously by Dahl and Blount.[18] The crystal packing diagram (Figure 2) and calculated bond distances (Table II) demonstrate that each $HFe_3(CO)_{11}^-$ is linked to two $H_2(i\text{-}Pr)_2N^+$ cations through two hydrogen bonds between O(12) and HN(2) on one cation and between O(14) and HN(1) on the other cation.

(18) Dahl, L. F.; Blount, J. F. *Inorg. Chem.* **1965**, *4*, 1373.

Table III. Carbonyl Stretching Frequencies of $[H_2R_2N][HFe_3(CO)_{11}]$

salt	lowest ν_{CO} (terminal) for solid[a] cm^{-1}	ν_{CO}(bridging), cm^{-1}					ν_{NH}(solid), cm^{-1}
		solid[a]	$CHCl_3$	benzene	THF	CH_3CN	
$[H_2Et_2N]$	1935	1550	1656	1640	1745	1725	3050
$[H_2(n\text{-}Bu)_2N]$	1927	1550		1641	1745		*c*
$[H_2(i\text{-}Pr)_2N]$	1883	1650	1665	1645	1745	1725	3220, 3065
$[HEt_3N]$	1912	1660	1640	1642[b]			3080
[PPN]		1720					

[a] In KBr. [b] A value of 1639 cm^{-1} was reported.[5] [c] Not observed.

The former hydrogen bond is a result of the interaction of one of the two protic hydrogens on the cation with the bridging CO group, while the latter is formed with one of the terminal CO groups. This connection also implies that each $H_2(i\text{-}Pr)_2N^+$ is bonded to two $HFe_3(CO)_{11}^-$ anions. Consequently, a chain structure is formed for the salt in the crystalline state.

The interaction between HN(1) and O(14) causes interesting variations in the iron–carbon bond distances on Fe(1) and Fe(2) centers. The Fe(1)–C(14) bond is slightly shorter than the corresponding Fe(2)–C(23) as a consequence of a higher degree of back-bonding from Fe(1) to C(14) induced by the HN(1)···O(14) hydrogen bond. In contrast, all other Fe(1)–C bonds are longer than the corresponding Fe(2)–C bonds. For comparison, the bond lengths from the bridging carbonyl carbon to Fe(1) and Fe(2) are 1.957 and 1.857 Å, respectively; the bond lengths of Fe(1)–C(13) and Fe(2)–C(24) trans to the bridging CO group are 1.845 and 1.822 Å, respectively; the distances of Fe(1)–C(11) and Fe(2)–C(21) trans to Fe(3) are 1.778 and 1.725 Å, respectively. Further analysis of the data in Table II indicates that the Fe–C bond distance trans to the bridging CO group is the longest while the Fe–C bond trans to Fe(3) is the shortest among the three terminal carbon–iron bonds in the Fe(1) and Fe(2) centers.

CO Frequency Change and Hydrogen Bond. The preceding X-ray structural results provide the basis for understanding the IR data of $[H_2(i\text{-}Pr)_2N][HFe_3(CO)_{11}]$. It is known that the bridging CO ligand of $HFe_3(CO)_{11}^-$ without contact interaction with its countercation absorbs at ca. 1740 cm^{-1}. The bonding between HN(2) and O(12) in the solid state accounts for the decrease of the absorption frequency to 1650 cm^{-1}. The other hydrogen bond between HN(1) and O(14) explains the observation of the unusual low terminal CO band at 1883 cm^{-1}. The electron density on the bridging CO is richer than that on the terminal CO groups. Thus, it is anticipated that the HN(2)···O(12) hydrogen bond is stronger than the terminal hydrogen bond. The bond distances of 1.932 Å for HN(2)–O(12) vs. 2.177 Å for HN(1)–O(14) seem to agree with such an expectation. The disappearance of the 1883 cm^{-1} band with little change in the bridging CO frequency in benzene and chloroform indicates that the weaker hydrogen bonding between HN(1) and O(14) is no longer present in the solutions, but the interaction between HN(2) and O(12) remains at approximately the same strength as in the solid state. The energy required for breaking the hydrogen bond between HN(1) and O(14) in these solutions is compensated at least partially by the large increase of entropy as the chain structure in the solid state is broken into monomeric contact ion pairs. In more polar solvents such as THF and acetonitrile, the hydrogen bond between HN(2) and the bridging CO is also broken in addition to the one between HN(1) and O(14) and the bridging CO frequency shifts to ca. 1740 cm^{-1}. The value agrees well with the bridging CO frequency of $(PPN)[HFe_3(CO)_{11}]$ (Table III) that has no contact interactions between the cation and anion in the solid state or in solutions. The complete absence of a hydrogen bond between $H_2(i\text{-}Pr)_2N^+$ and $HFe_3(CO)^-_{11}$ in THF may be attributed to the great solvation power of this solvent to the salt, especially to $H_2(i\text{-}Pr)_2N^+$ that is capable of forming two hydrogen bonds with the donor atoms of the solvent molecules.

The variation of the bridging CO frequencies of the $H_2Et_2N^+$ and $H_2(n\text{-}Bu)_2N^+$ salts with the environments could also be understood in terms of the number of hydrogen bonds to the bridging CO group. The unusual low absorption frequency of 1550 cm^{-1} in the solid state may be rationalized on the basis of a specific interaction as shown in 1 between the bridging CO and the countercation

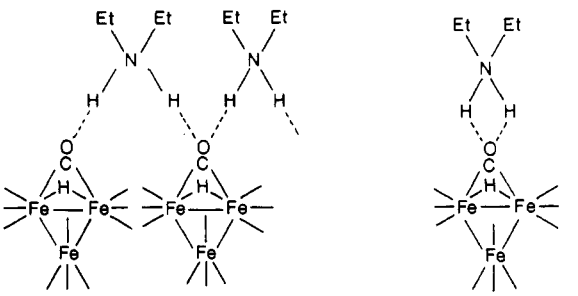

1 2

leading to the formation of two hydrogen bonds for each bridging CO. The nonbonded electrons on the oxygen atom or the π-electron density across the bridging CO could serve as the electron sources for such hydrogen bonding. An alternative structure, 2, in which $H_2R_2N^+$ acting as a chelating group could also account for the low frequency of the bridging CO. However, it is considered less likely because of the unfavorable hydrogen bond angles. In solution, the $H_2Et_2N^+$ and $H_2(n\text{-}Bu)_2N^+$ salts behave similarly to the $H_2(i\text{-}Pr)_2N^+$ salt as indicated by the IR data shown in Table III and Figure 3. An increase of the bridging CO frequency from 1550 cm^{-1} in the solid state to ca. 1650 cm^{-1} in benzene or chloroform indicates that the chain structure as given in 1 is destroyed in these solutions, but only one of the two hydrogens on $H_2R_2N^+$ is still bonded to the bridging CO. A further shift of the CO frequency to ca. 1730 cm^{-1} in THF and acetonitrile implies that both hydrogen bonds existing in the solid state are all broken in these solutions.

Conclusions

We have demonstrated that the interaction sites of $HFe_3(CO)_{11}^-$ with dialkylammoniums in the solid state change dramatically with the alkyl substituent on the cations. The structural difference between the $H_2(i\text{-}Pr)_2N^+$ and $H_2R_2N^+$ (R = Et, *n*-Bu) salts in the crystalline state is probably caused by a steric effect during crystal packing. Presumably, it is less likely for the two bulkier $H_2(i\text{-}Pr)_2N^+$ cations to be sufficiently close to a bridging CO to form two hydrogen bonds without causing severe steric interference. For all the dialkylammonium salts listed in Table III, two hydrogen bonds exist between the anion and the

countercations in the solid state, while only one or none is present in solution. In all cases, it is interesting to point out that the frequency of the bridging CO decreases approximately by 100 cm^{-1} for each hydrogen bond formed to this CO group.

Acknowledgment. We thank the National Science Council of the Republic of China for support of this work.

Registry No. $[H_2Et_2][HFe_3(CO)_{11}]$, 56048-18-1; $[H_2(n\text{-}Bu)_2N][HFe_3(CO)_{11}]$, 107011-15-4; $[H_2(i\text{-}Pr)_2N][HFe_3(CO)_{11}]$, 107011-16-5; $[PPN][HFe_3(CO)_{11}]$, 23254-21-9; $[HEt_3N][HFe_3(CO)_{11}]$, 56048-18-1; $K[HFe_3(CO)_{11}]$, 87145-35-5; CO, 630-08-0.

Supplementary Material Available: Table IV, fractional coordinates ($\times 10^4$) for the hydrogen atoms of $[H_2(i\text{-}Pr)_2][HFe_3(CO)_{11}]$, and Table V, anisotropic temperature factors of $[H_2(i\text{-}Pr)_2N][HFe_3(CO)_{11}]$ (2 pages); Table VI, observed and calculated structure factors (14 pages). Ordering information is given on any current masthead page.

Reaction of $Fe(\eta^5\text{-}C_5H_4PPh)(\eta^5\text{-}C_5H_4)$ with LiC_5H_5 and $NaFe(CO)_2(\eta^5\text{-}C_5H_5)$. Structures of $\{Fe[(\eta^5\text{-}C_5H_4)_2]P(C_6H_5)\text{-}P\}Fe(H)(\eta^5\text{-}C_5H_5)(CO)$ and $\{(C_6H_5)[Fe(\eta^5\text{-}C_5H_5)(\eta^5\text{-}C_5H_4)][Fe(\eta^5\text{-}C_5H_5)(\eta^5\text{-}C_5H_3C(O))]P\text{-}P,C\}Fe(\eta^5\text{-}C_5H_5)(CO)\cdot CHCl_3$

Ian R. Butler, William R. Cullen,* and Steven J. Rettig[1]

Department of Chemistry, The University of British Columbia, Vancouver, British Columbia, Canada V6T 1Y6

Received September 2, 1986

Crystals of $\{Fe[(\eta^5\text{-}C_5H_4)_2]P(C_6H_5)\text{-}P\}Fe(H)(\eta^5\text{-}C_5H_5)(CO)$ (**17**) are monoclinic, space group $P2_1/c$, with a = 13.521 (2) Å, b = 10.998 (1) Å, c = 13.007 (2) Å, β = 101.375 (7)°, and Z = 4, and crystals of $\{(C_6H_5)[Fe(\eta^5\text{-}C_5H_5)(\eta^5\text{-}C_5H_4)][Fe(\eta^5\text{-}C_5H_5)(\eta^5\text{-}C_5H_3C(O))]P\text{-}P,C\}Fe(\eta^5\text{-}C_5H_5)(CO)\cdot CHCl_3$ (**12**) are monoclinic, space group $P2_1/c$, with a = 11.878 (1) Å, b = 11.980 (1) Å, c = 22.948 (2) Å, β = 103.743 (7)°, and Z = 4. Both structures were solved by heavy-atom methods and were refined by full-matrix least-squares procedures to R values of 0.048 and 0.045 for 1922 and 3481 reflections, respectively. Compound **17** is a derivative of $(\eta^5\text{-}C_5H_5)Fe(CO)_2H$ in which a carbonyl group has been replaced by the phosphine $Fe[(\eta^5\text{-}C_5H_4)_2]P(C_6H_5)$. The structure of **12** is related to that of **17** in that the phosphine ligand is a derivative of diferrocenylphenylphosphine in which one of the ferrocene groups is substituted by a -C(O)- group that also constitutes the X group in $(\eta^5\text{-}C_5H_5)Fe(CO)PR_3X$. Bond distances in both structures are similar to those in related molecules. **17** was isolated following treatment of (1,1′-ferrocenediyl)phenylphosphine (**1a**) with $NaFe(CO)_2(\eta^5\text{-}C_5H_5)$. Cleavage of the [1]ferrocenophane (**1a**) with LiC_5H_5/TMED affords $FcPPh(C_5H_5)$ (**3**). Solutions containing **3** and LiC_5H_5 react with $IFe(CO)_2(\eta^5\text{-}C_5H_5)$ to yield separable diastereomers of **12**.

Much of our current research has focused on the cleavage reactions of phosphorus- or arsenic-bridged [1]-ferrocenophanes using alkyl- or aryllithium reagents[2,3] (Scheme I). We have also explored the subsequent reaction of the resulting lithium compounds (e.g. **2a**, R = Ph) with appropriate transition-metal derivatives.[4,5] For example, the reaction of $Fe(CO)_2(\eta^5\text{-}C_5H_5)I$ with **2a**, R = Ph, results in the formation of the phosphorus-coordinated compound **5a** as the major reaction product together with smaller amounts of the CO migration product **6a**.[4] The analogous reaction of **2b**, R = Ph, gives only the arsenical **4b** at ambient temperature; however, heating solutions of **4b** results in the formation of **5b**.[6]

Scheme I

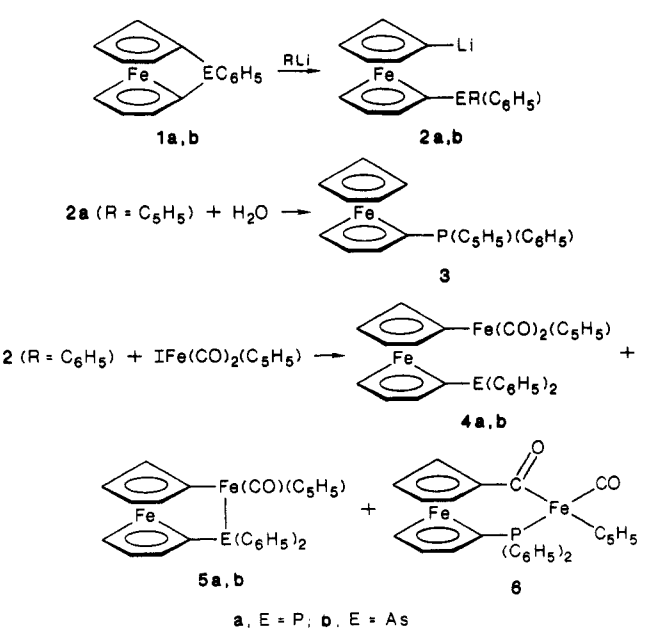

(1) Experimental Officer, U.B.C. Crystal Structure Service.
(2) Seyferth, D.; Withers, H. P. *Organometallics* **1982**, *1*, 1275.
(3) Butler, I. R.; Cullen, W. R. *Can. J. Chem.* **1983**, *61*, 147.
(4) Butler, I. R.; Cullen, W. R. *Organometallics* **1984**, *3*, 1846.
(5) Butler, I. R.; Cullen, W. R.; Einstein, F. W. B.; Willis, A. J. *Organometallics* **1985**, *4*, 603.
(6) Recent results show that **4b** transforms to **5b** on heating in toluene solution (110 °C). **5b**: ^1H NMR ($CDCl_3$, 270 MHz) δ 3.85 (m, 1), 4.02 (m, 1), 4.16 (m, 1), 4.22 (m, 1), 4.40 (2m, 2), 4.50 (s, 5), 4.63 (m, 1), 4.70 (m, 1), 7.45–7.50 (m, 6), 7.55–7.63 (m, 4); MS (150 °C), m/e 563 (2.93), 562 (M^+, 8.68), 535 (12.38), 534 (36.41), 456 (14.11), 414 (28.31), 381 (4.56), 337 (36.91), 305 (66.96), 304 (82.95).

0276-7333/87/2306-0872$01.50/0